Journal of Zhejiang University-SCIENCE A (Applied Physics & Engineering)
ISSN 1673-565X (Print); ISSN 1862-1775 (Online)
www.zju.edu.cn/jzus; www.springerlink.com
E-mail: jzus@zju.edu.cn

Numerical modeling of an advancing hydraulically-driven pile in sand

Meen-wah GUI

(*Department of Civil Engineering, National Taipei University of Technology, Taipei 106, Taiwan*)

E-mail: mwgui@ntut.edu.tw

Received Apr. 6, 2010; Revision accepted July 15, 2010; Crosschecked Oct. 12, 2010

Abstract: The penetration of a model pile through sand was investigated via a numerical analysis. Data from nine triaxial compression tests on dense specimens at different stress levels was generalized and used to create an empirical non-linear plastic hardening stress-strain relation for use in the analysis. As the computer program used is capable of large displacement analyses in radial symmetry, we expected that the analysis would easily reproduce the tip resistance penetration profile of the model pile in sand of known density and stress. However, initial attempts led to over-prediction. Successful analyses required both successive reformations of the mesh and the complete elimination of the dilatant peak in soil strength, which is naturally eliminated under large confining stress directly beneath the advancing tip, and that soil in the far-field had strained insufficiently to reach peak strength. Thus, the soil around the shaft must have been sheared to a critical state as it flowed past the tip. The hypothesis that the resistance to displacement piles in sand is mainly a function of the deformability of the sand was again proven, and the use of peak strength in the traditional bearing capacity formulae was found to be inappropriate. Independent investigation in this direction is needed to quantify the hypothesis.

Key words: Hydraulic pile, Tip resistance, Sand, Double yield (DY) model, Pile penetration, Grid re-meshing
doi:10.1631/jzus.A1000144 **Document code:** A **CLC number:** TU67

1 Introduction

It is common for engineers to attempt to predict pile bearing capacity following the method of Terzaghi and Peck (1948), i.e., using bearing capacity coefficients. The difference in resistance between dense and loose sands is then explained by their different angles of friction. However, this approach does not seem to be justifiable. For example, engineers have tried unsuccessfully to apply the conventional bearing capacity theory to pile design in calcareous sands, which are characterized by high angles of friction (>40°) and extremely high crushability (Kuwajima *et al*., 2009). The use of such an incomplete theory has sometimes led to very costly disasters and remedial work. According to Schofield (2005), the bearing capacity theory is incorrect because it ignores soil compressibility and therefore is not representative of actual conditions. Salgado *et al.* (2004) have also commented that most of the terms used in the bearing capacity equation are only empirical and that uncertainties have always existed regarding the equation. Large safety factors have been used, in part to account for such uncertainties.

The problem is compounded by many difficulties in penetration analysis of displacement piles in sand, such as the need to have a constitutive model that is able to represent the hardening and softening of the material, and a numerical procedure that can model large strain deformations and appropriate boundary conditions. Field-testing is not generally suitable for validating theoretical solutions because of soil variability and because there are so many unknown quantities associated with a field test (Yu and Mitchell, 1998; Gui and Muhunthan, 2006; Gui and Jeng, 2009; Zhou *et al.*, 2009). Only by using model

tests with sand of known properties and a constitutive model that can accurately reproduce the soil stress-strain properties can statements be made about more subtle influences such as post-peak softening in rupture bands. However, no fundamental constitutive model can yet reproduce the range of soil behavior invoked in a pile penetration.

The objective of this study was to investigate the conditions evolving around an advancing hydraulically-driven pile by using appropriate soil data directly in a numerical analysis of centrifuge model tests and to compare numerical and experimental models of penetration. The effects on tip resistance of stiffness in the far field at low strain and stress levels, strength in the medium far field with dilatancy at middling stress levels, and volumetric contraction due to crushing under high stress levels in the near field, were assessed. The pre-peak behavior of Fontainbleau sand was fitted using an elementary cap model of elastic-plastic soil behavior, which is available in the computer program Fast Lagrangian Analysis of Continua (FLAC) (Itasca Consulting Group, Inc., 2005). A technique was therefore established that could reproduce triaxial stress-strain data up to peak strength over a very wide range of stresses (0.1 to 30 MPa). Although this might well be described as only a little more than curve-fitting, it permitted an investigation of the remaining issues of large strain analysis and post-peak softening.

2 Centrifuge tests

Centrifuges have been widely adopted in modeling geotechnical problems because they enable the behavior of a foundation to be observed in a soil specimen of known parameters, without the expense and delay of full-scale tests. A miniature hydraulic pile used in a centrifuge test can be treated as a hydraulically-driven pile with a 60° pile shoe, since a standard analysis would require the dimensions of the test specimen to be scaled up according to the acceleration level while preserving the density of the soil. A 10 mm diameter pile will model a 700 mm diameter prototype circular pile at an acceleration level of 70*g*.

The model pile results used here were obtained by Bolton *et al.* (1999) from testing at the centre of a 850 mm diameter container. The test specimen was prepared by hand pluviating Fontainbleau sand (d_{50}=0.18 mm, where d_{50} is the grain diameter at which 50% of the soil weight is finer) from a single-hole hopper into the container to a height of 350 mm. It was considered a normally consolidated specimen as no preloading of the specimen was carried out before the test. The inferred value of d_{50} of Fontainbleau sand was 0.181 mm. The coefficient of uniformity (d_{60}/d_{10}) of the sand was 1.69, where d_{60} and d_{10} is the grain diameter at which 60% and 10% of the soil weight is finer, respectively. The average values of maximum and minimum void ratios were 0.55 and 0.92, respectively. Hence, the calculated initial relative density of the specimen used was about 89%. The relative density after swing up remained about the same (89.4%), as the specimen was very dense, and thus significant densification could not take place. The model pile was hydraulically driven to a prototype depth of about 16 m at a nominal rate of 3.6 mm/s in the centrifuge. A load cell, located at the shoulder of the pile tip, was used to measure the tip resistance while a potentiometer was used to measure the depth of penetration, which was the distance between the surface of the specimen and the shoulder of the tip. The results obtained were highly repeatable and that tests carried out independently by four other laboratories under similar test conditions showed that the intra-laboratory results varied only by a maximum of 15% (Bolton *et al.*, 1999). The tip resistance and depth data have been used as a standard against which numerical analyses of sand penetration by prototype piles are compared.

3 Soil model and its parameters

3.1 Soil parameters of double yield model

The FLAC is an explicit finite difference program intended for modeling non-linear material behavior. The double yield (DY) model in FLAC allows the user to represent arbitrary non-linear hardening and softening of the material based on a Mohr-Coulomb elasto-plastic model with a non-associated flow rule. Parameters are given in terms of the variation with plastic shear strain of the apparent cohesion c', angle of friction ϕ', and angle of dilation ψ', all defined with respect to envelopes of Mohr

circles. To cater for volumetric compaction, a volumetric yield function with an associated flow-rule is also incorporated. Detailed discussion of the formulation of the DY model can be found in FLAC.

3.2 Fit to triaxial tests

Since the tip resistance is stress level dependent, it is important to assign different soil properties to different soil elements. A method of generalization of triaxial data into high-, medium-, and low-stress zone (H-, M-, and L-stress zone) was used here. Initially, the soil was modeled as elastic; following yield, an empirical plastic hardening curve was defined for deviatoric stress and strain in each triaxial test. Simple (c', ϕ') strength envelopes were fitted at several deviatoric strain levels, which permitted the program to select appropriate mobilized plastic strengths. Different envelopes were used for H-, M-, and L-stress magnitude, so that the curved strength envelopes were idealized as tri-linear.

An example is demonstrated here using the triaxial data produced by Luong and Touati (1983) using 95% dense Fontainbleau sand. Data points for shear strains ε_q at 0.5%, 1.0%, 2.0%, 4.0%, 8.0%, and 16.0% were extracted and plotted in a (q, p') space (Fig. 1a). Each of the (q, p') curves in Fig. 1a had a unique shape (Fig. 1b). This unique shape shows that we could divide all the triaxial data into three stress zones: high, medium and low.

The H-stress zone was defined by q, p' data from a test with confining pressures $\sigma_3 \geq 6$ MPa (in this case 6, 16 and 30 MPa), to which the best straight line was fitted. The M-stress zone was treated similarly using data between 0.5 and 6 MPa (in this case 0.5, 2, 4 and 6 MPa), and the L-stress zone was fitted using lines drawn between the origin and the data of the 0.5 MPa test. Having divided the data into three zones, we could define:

$$q = \Omega + \eta \cdot p', \tag{1}$$

where η is the gradient of the q-p' line, $q=\sigma_1-\sigma_3$, $p'=(\sigma_1+2\sigma_3)/3$, and Ω is the apparent deviatoric stress. For a triaxial compression test, the mobilised angle of friction ϕ' with respect to a particular strain level can be calculated:

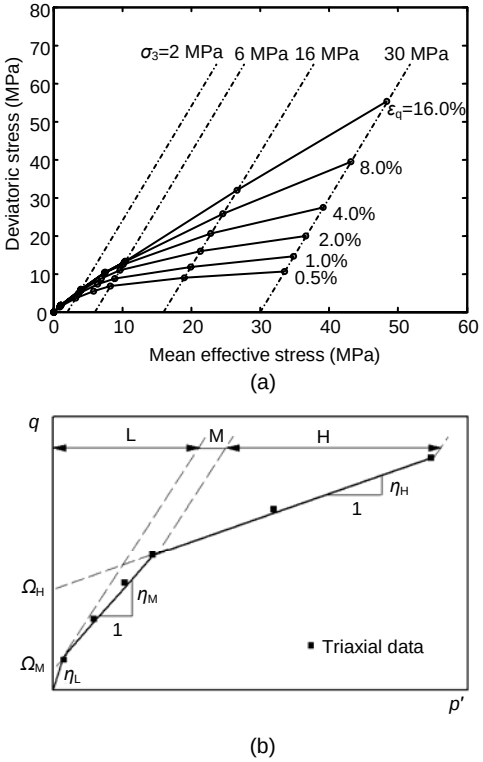

Fig. 1 Triaxial data plotted for a particular strain level (a) and definition of η and Ω for three different stress zones in a typical q-p' plot (b)

$$\phi' = \sin^{-1}\left(\frac{3\eta}{6+\eta}\right). \tag{2}$$

Using the relationship between the major σ_1 and minor σ_3 principal stresses, Eq. (3), we can obtain the 'arbitrary' cohesion intercept c':

$$\sigma_1 = \sigma_3 \tan^2\left(45° + \frac{\phi'}{2}\right) + 2c' \cdot \tan\left(45° + \frac{\phi'}{2}\right), \tag{3}$$

$$c' = \frac{\Omega}{2\tan\left(45° + \frac{\phi'}{2}\right)\left(1 - \frac{\eta}{3}\right)}. \tag{4}$$

Armed with Eqs. (2) and (4), the relationship between ϕ' and c' can be calculated. The dilation angle ψ' is taken to be (Bolton, 1986)

$$\psi' = \phi' - 32°, \tag{5}$$

though it was recognized that regression lines could

separately have been fitted to the various data of volumetric strains from the various triaxial tests in the same way as used to define c' and ϕ'.

The second yield function was the volumetric plastic hardening of the cap. Because of the limitation of the cap model in FLAC, no plastic volume loss would be predicted during a constant-p' test on normally consolidated soil. This conflicts with reality. We decided to select the plastic volume change after both the consolidation and shear stages of the tests, for entry into the model. The consequence was that we would overestimate volume loss during isotropic consolidation, and then underestimate volume loss during shear. However, soil reaching a critical state should be modeled reasonably well with respect to overall volume change.

The elastic Young's moduli measured from the triaxial tests were 48 MPa, 1.86 GPa and 6.8 GPa for L-, M- and H-stress zone, respectively. The effect of Poisson's ratio ν on the collapse load was negligible (van den Berg, 1994); hence, a constant value of 0.25 was adopted.

3.3 Back analysis of triaxial tests

Seven triaxial simulation analyses were performed using FLAC. The confining pressure ranged from 100 kPa to 30 MPa. Only half of the sample was modeled and it was divided into 50 elements (5×10). The top and bottom platens were fixed in both X and Y directions. A strain-controlled test at a rate of 5×10^{-5} m/step was then applied to the sample. The variations in the angle of friction and the apparent cohesion with plastic strain for H-, M-, L-zone used in the analysis are shown in Figs. 2a and 2b, respectively. In addition, the non-linear volumetric strain loading curve is shown in Fig. 3.

Three FLAC results (one for each of the high, medium and low pressure tests) together with the corresponding experimental results from Luong and Tuoati (1983) are shown in Figs. 4a and 4b. The FLAC normalized deviatoric stress q/σ_3 versus shear strain ε_q profiles compared well with the experimental profiles for all the tests (Fig. 4a). The maximum deviation in normalized deviatoric stress q/σ_3 observed was no more than 20% for the high pressure test and 10% for the medium and low pressure tests.

For the prediction of volumetric strain ε_v, as expected, the results match only in a global sense. The FLAC ε_v versus ε_q profiles compared reasonably well with the experimental profiles for high and medium pressure tests at the ultimate value (Fig. 4b). For low pressure tests, FLAC managed to predict both the contraction and dilation of the specimen though it

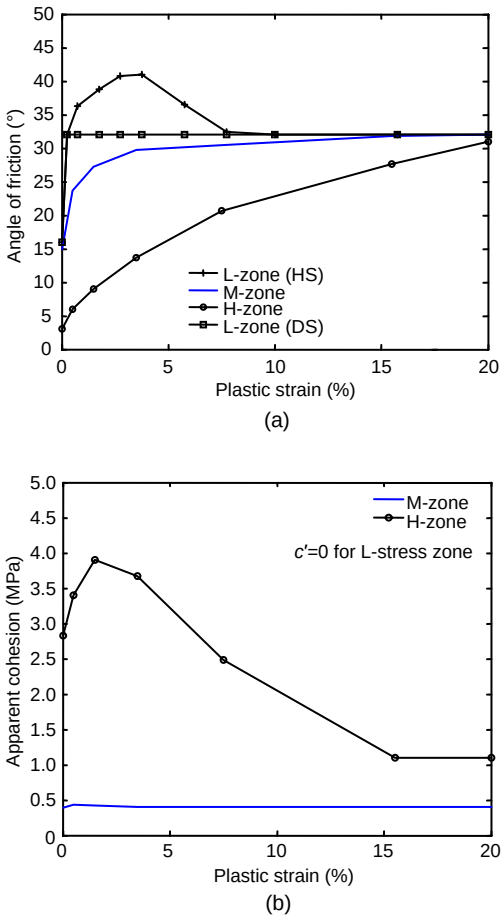

Fig. 2 Variation of angle of friction (a) and apparent cohesion (b) with plastic strain for H-, M-, L-zone

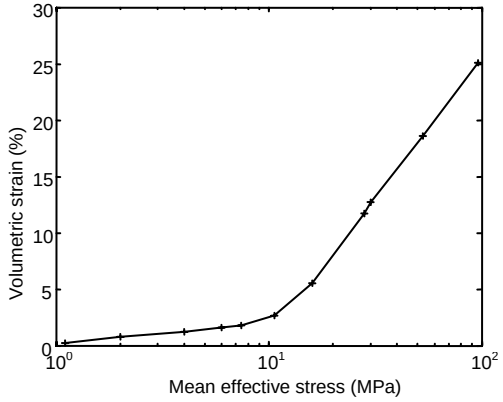

Fig. 3 Variation of volumetric strain and mean effective stress

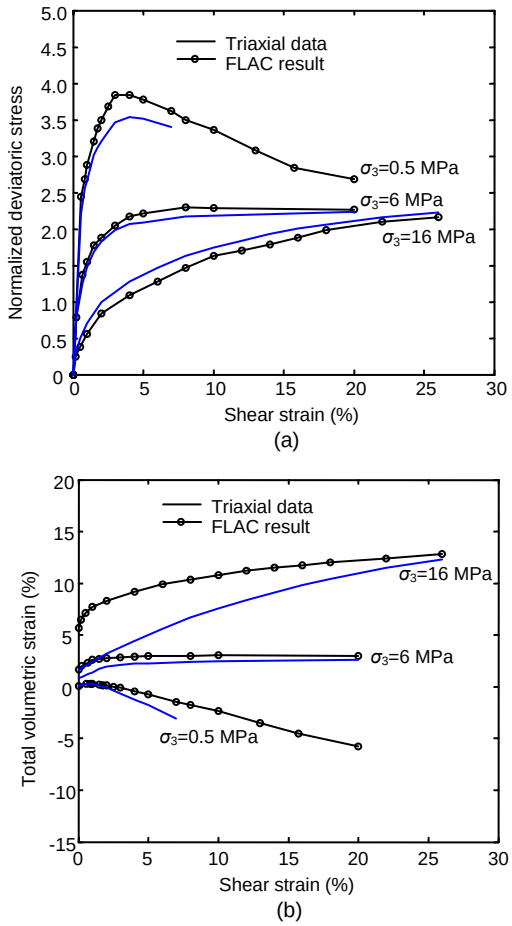

Fig. 4 Comparison of numerical and experimental results
(a) Normalized deviatoric stress; (b) Total volumetric strain. Triaxial data were conducted by Luong and Tuoati (1983)

underestimated the dilation by about 50%. Clearly, not all the subtleties of the influence of grain crushing on soil dilation have been captured. Nevertheless, this approach in the DY model of FLAC has been shown to be able to give good back analyses of the experimental triaxial compression tests results.

4 Modeling of pile penetration

4.1 Modeling parameters

The continuous penetration of a 0.7 m diameter prototype pile with a 60° apex angle pile tip was modeled using the following analysis. To represent the prototype boundary conditions in the centrifuge, a finite difference grid of 30 m wide by 25 m high (Fig. 5) was adopted. No lateral movement was allowed at the side boundaries while both vertical and lateral movements were prevented at the base.

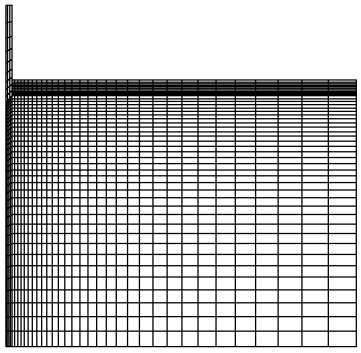

Fig. 5 Finite difference mesh used in the analysis

Before the penetration process began, interface elements that were characterized by Coulomb sliding were created between the pile and the soil to account for the frictional interface behavior, to simulate the relative slip between the soil and the shaft after a limiting stress condition is reached. The roughness angle δ of the pile-soil interface was obtained by shearing the sand resting on a piece of pile material in a direct shear box apparatus. Although the roughness angle was found to decrease (from 20° to 15°) non-linearly with the increase in normal stress (from 10 to 400 kPa), a constant value of 15° was adopted in the analysis because of high stresses around the shaft.

All the elements in an FLAC analysis must be attributed to one of the three H-, M-, L-stress zone. The idealized stress zones around a pile and the stress-state of the soil elements are illustrated in Fig. 6. Points A, B and C correspond to each of the stress zones and the corresponding stress-stain curves are shown in the bottom left corner of Fig. 6. Near the tip, at point A, the mean effective stress was very high and the soil must have been subjected to a very large shear strain. At the far-field, point C, the mean effective stress was low and the soil was subjected to a smaller shear strain. The penetration process was then modeled by prescribing an incremental displacement to the rigid pile body. The incremental displacement, or numerical step size, together with the grid size have significant effects on the numerical result. These effects have been eliminated by providing an incremental displacement or numerical step size of 2.5×10^{-5} m/step and a very fine mesh around the tip (Fig. 5).

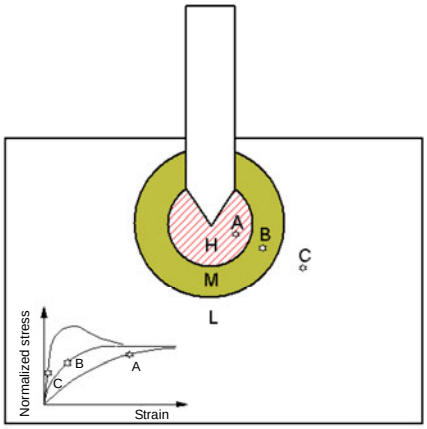

Fig. 6 Idealized stress bulb and stress states of soil in the vicinity of pile tip

Because of the very large changes in geometry at the outset of a fresh penetration from the surface of the ground, the probe had to be started in a 1.5 m deep semi pre-bored-hole. In the field, penetration of a pile would cause the soil along the shaft to expand as a cylindrical cavity, which would then alter the radial stress of the soil. To model the field situation as closely as possible, analysis with a pre-bored-hole with a sectional area of one quarter of the actual pile was used to minimize this effect. The hole was then expanded to actual size of the pile following the penetration process. The penetration process was modeled using the updated Lagrangian technique where the mesh was automatically updated during the FLAC analysis. The conservation of energy law was applied in the formulation of FLAC, thus, there was no loss of energy during the penetration modeling.

4.2 Grid re-meshing analysis

We thought that the Lagrangian approach adopted in FLAC was a realistic way of modeling the penetration problem. However, the FLAC analysis was limited by the criterion that the rectangular grid must not deform excessively, otherwise the analysis would be terminated by FLAC because of an internal error (Itasca Consulting Group, Inc., 2005). As the penetration of a pile is a large strain problem, large local deformations cannot be avoided and elements will inevitably be subjected to excessive distortion, and thus interrupt a complete analysis.

To prevent the geometry distortion problem, it was necessary to re-mesh the grid just before the internal error was about to be encountered. After advancing the pile downward for some distance, 0.1 m in this case, the analysis recorded the stresses of all the elements and re-meshed the grid. Unlike finite element analyses that store the stresses of an element at certain interpolation points, FLAC stores the stresses of an element at the geometrical centre of the element itself. After a re-meshing process, the same element would still have the same stresses but at a slightly different geometrical centre (Fig. 7). It was then necessary to redistribute these stresses for the new mesh obtained.

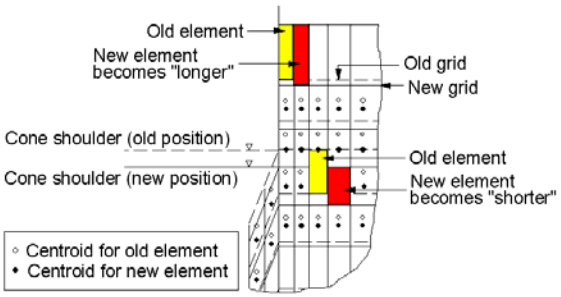

Fig. 7 Geometry of finite difference grid before and after re-meshing

4.3 Updating element stresses

The stresses of the elements were redistributed using the method of inverse distance weighting (Shepard, 1968). It is a common method for multivariate interpolation, which is a process for assigning values to unknown points using values from a scattered set of known points. The generic inverse distance weighting equation used is

$$\sigma_{x,y}=\sum_{i=1}^{n} w_i\sigma_i \Big/ \sum_{i=1}^{n} w_i, \tag{6}$$

where $\sigma_{x,y}$ is the stress to be estimated, σ_i represents the stress control value for the ith sample point, and w_i is the weight that determines the relative importance of individual stress control point σ_i in the updating procedure. To allow near points more influence than distant points, an inverse of distance to a power was used:

$$w_i=\frac{1}{d_{x,y,i}^{p}}, \tag{7}$$

where $d_{x,y,i}$ is the distance between $\sigma_{x,y}$ and σ_i, and p is a power defined by the user. As a result, the weight

decreases as distance increases from the interpolated points. The most common value of p is 2, which was also used in this analysis.

After redistributing the stresses, the subsequent penetration process was modeled and the re-meshing procedure repeated. Because FLAC assigns stresses of an element to the geometrical centre of that element, the total number of elements must be kept unchanged every time the re-meshing procedure is performed. As a result, after a few meters of penetration, the elements below the shoulder of the pile would become shorter and shorter while the elements above the shoulder would become longer and longer (Fig. 7). We considered this to be acceptable as we were interested in computing the tip resistance of the pile, rather than the shaft resistance. However, we recommend that this effect be studied in the future.

4.4 Validation of re-meshing technique

This re-meshing procedure was validated using an example of cavity expansion of a thick-walled cylinder in a medium characterized by the Mohr-Coulomb plasticity model. The cylinder had inner and outer radii of 1.0 and 10.0 m, respectively. The properties of the material are as follows: density is 2500 kg/m^3, shear modulus is 0.28 GPa, bulk modulus is 0.39 GPa, apparent cohesion is 3.45 kPa, friction angle is 30°, and zero dilation angle. An isotropic in situ stress state was assumed to exist with stresses equal to 30 MPa. In the first analysis, the grid was allowed to deform naturally; in the second analysis, the grid was re-meshed after about every 0.025 m of deformation. The configuration of the thick-walled cylinder and the boundary conditions used in the analysis are shown in Fig. 8. Comparisons between the normalized tangential stresses obtained from the analytical solution (Salencon, 1969) together with the two FLAC analyses, with and without re-meshing, are also presented in Fig. 8. The analysis without re-meshing consistently overestimated the analytical result by about 2%. The analysis using the re-meshing technique underestimated the analytical solution by about 8.5% at a distance of 0.5 m from the cavity wall (1.5 m from the center line (C.L.)) but the underestimation gradually decreased in a non-linear fashion to 0% at a distance of 7 m from the cavity wall. Though more rigorous validations may be needed, it can be concluded that this re-meshing procedure could also produce a reasonable result.

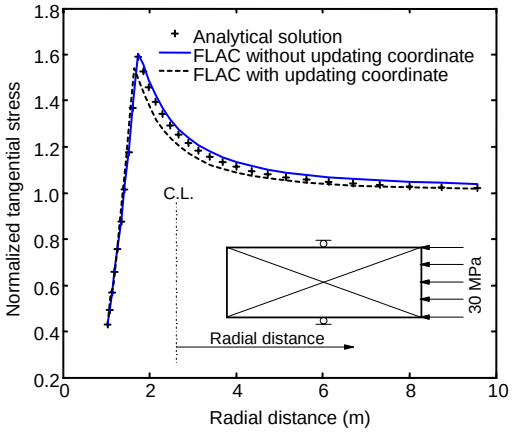

Fig. 8 Comparison of the tangential stress derived from various analyses for the validation of the grid re-meshing technique

5 Results and discussion

The schematic stress-strain curves (idealized from Fig. 2a) used for the H-, M-, L-zone are shown in Fig. 9. For H- and M-zone only one type of stress-strain curve was employed. However, for the L-zone, two possible types of stress-strain curve models (strain hardening/softening (HS) and dilation-suppressed (DS)) were adopted in the analysis.

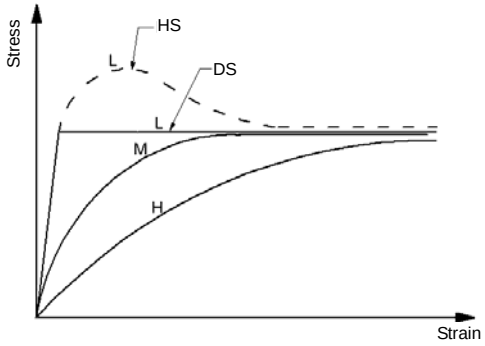

Fig. 9 Stress-strain relationships used for the H-, M-, L-zone

5.1 Strain hardening/softening behavior

The FLAC results using the strain HS model and the tip resistance profile from a centrifuge test on dense (relative density is about 90%) Fontainbleau sand are plotted in Fig. 10 (profile 'HS'). In general, the FLAC produced a similar shape of profile to that obtained in the centrifuge. The predicted tip resistance profile for the first 12.3 m of penetration was no more than 40% above the experimental result. After a depth

of 12.3 m, the numerical profile diverged quickly from the profile to 1.4 times the centrifuge result.

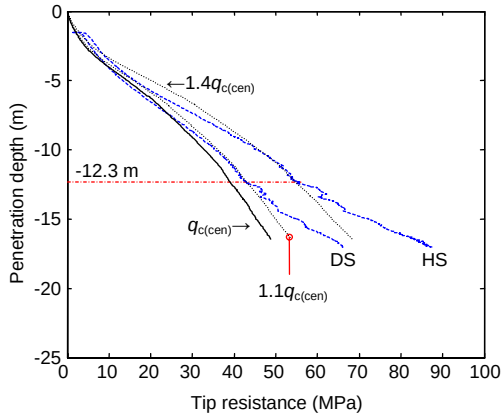

Fig. 10 Comparison of experimental $q_{c(cen)}$ and numerical q_c profiles obtained using strain HS and DS soil models

5.2 Dilation-suppressed behavior

The overestimation of the tip resistance could be due to the elements beneath the pile tip not being subjected to a true triaxial condition, making the triaxial data unrepresentative of the true strength of the soil. According to Mair and Wood (1987), only the soil elements directly beneath the pile tip are equivalent to vertical soil samples (i.e., conventional triaxial samples taken from the ground with their axes vertical). Other elements are equivalent to inclined samples, and the expected anisotropy of the soil will therefore influence the pile results. Laboratory results obtained by Tatsuoka *et al.* (1986) clearly indicate the effect of anisotropy on the measured angle of friction ϕ'. However, other effects must first be accounted for in the analysis.

Further to this effect of anisotropy, Lee (1990) observed rupture planes that developed at intervals along the 700 mm diameter prototype pile. The rupture planes indicated that the zone around the penetrometer shaft was being disturbed and subjected to lower shear stress during the penetration process (Fig. 11). Because of the inherent complexity of the rupture zone that is associated with anisotropy, and as a possible scenario, it might be appropriate simply to use a DS model in the FLAC analysis.

By adopting a DS model, this possible scenario shows that the computed results (profile 'DS' in Fig. 10) now overestimate the centrifuge result by only 10%. The lower overestimation was expected because the reduced strength on bedding planes

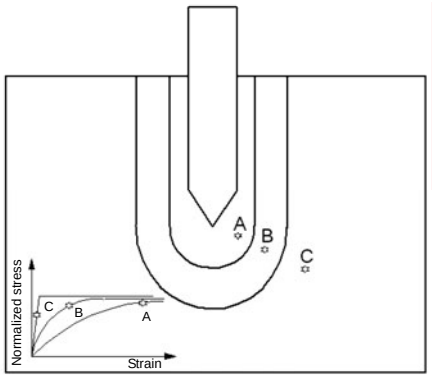

Fig. 11 Idealized mobilized stress states in the vicinity of an advancing pile

would have reduced the penetration resistance. As in the case of the strain HS model, after a penetration depth of 12.3 m, the numerical profile diverged quickly from the profile of 1.1 times the centrifuge result. Note that the rates of divergence in both the 'HS' and 'DS' profiles were almost equal. This could be due to the imperfect grid geometry created after such a long penetration depth (12.3 m), as mentioned above. However, the result of the DS model for the first 12.3 m of penetration is likely to be accepted as excellent from the viewpoint of a geotechnical engineer as the margin of deviation from the experimental result was only 10%.

6 Implications for design

FLAC analyses have shown that, because of soil anisotropy and the development of rupture planes, even dense sand does not have, at any point around a deep pile, an angle of friction greater than the critical angle of friction ϕ'_{crit}, which is the strength observable at larger strains in loose sand. If a bearing capacity formula had to be applied, the mean strength parameter would have to be some sort of 'reduced' angle of friction. The idea of using a 'reduced' angle of friction has previously been adopted by various researchers. For example, Graham and Hovan (1986) pointed out that the critical angle of friction ϕ'_{crit} could be used in the design of large footings for offshore structures. However, the reason for adopting a ϕ'_{crit} design was not explained. Collins *et al.* (1992) used the average value between the peak and critical angles of friction while Randolph *et al.* (1994) also adopted ϕ'_{crit} analysis in predicting the end-bearing capacity of driven piles in sand. Yasufuku and Hyde (1995)

suggested that the pile end-bearing pressure in crushable sands is a function of the reduced secant friction angle, and that the settlement at which the bearing capacity is mobilized increases with soil compressibility. Their reduced secant friction angle is given by $\arctan\left[\frac{2}{3}\tan\phi'_{\text{sec}}\right]$.

It is in this direction that progress must be made, but soil compliance must be recognized as a function of stress level. In the meantime, engineers need to be very careful in selecting the value of the angle of friction to be used in the bearing capacity formulae for their pile foundation design.

7 Conclusions

The FLAC was used in modeling the advancement of a penetrating pile, which required re-meshing and softening in zones that were believed to have ruptured. No element of soil mobilized more than the DS critical state angle of friction. Based on both the physical and numerical analyses, we conclude that attempts to correlate pile tip resistance with the peak angle of friction of sand using the bearing capacity formulae must be discouraged and an alternative approach, relating penetration resistance to soil deformations (not strength) at various stress levels, should be sought. Further research in this direction is strongly recommended.

Acknowledgements

The author is grateful to Dr. Noriko KODAMA of Waseda University, Japan for her enthusiastic help in the re-meshing technique.

References

Bolton, M.D., 1986. The strength and dilatancy of sands. *Geotechnique*, **36**(1):65-78.

Bolton, M.D., Gui, M.W., Garnier, J., Corte, J.F., Bagge, G., Laue, J., Renzi, R., 1999. Centrifuge cone penetration test in sand. *Geotechnique*, **49**(3):543-552.

Collins, I.F., Pender, M.J., Wang, Y., 1992. Cavity expansion in sands under drained loading conditions. *International Journal for Numerical and Analytical Methods in Geomechanics*, **16**(1):3-23.

Graham, J., Hovan, J.M., 1986. Stress characteristics for bearing capacity in sand using a critical state model. *Canadian Geotechnical Journal*, **23**(2):195-202. [doi:10.1139/t86-029]

Gui, M.W., Muhunthan, B., 2006. Bearing capacity of foundations on sand using the method of slip line. *Journal of Marine Science and Technology*, **14**(1):1-14.

Gui, M.W., Jeng, D.S., 2009. Application of cavity expansion theory in predicting centrifuge cone penetration resistance. *The Open Civil Engineering Journal*, **3**(1):1-6. [doi:10.2174/1874149500903010001]

Itasca Consulting Group, Inc., 2005. Fast Lagrangian Analysis of Continua Version 5.0 User Manual. Minneapolis, USA.

Kuwajima, K., Hyodo, M., Hyde, A.F.L., 2009. Pile bearing capacity factors and soil crushability. *Journal of Geotechnical and Geoenvironmental Engineering*, **135**(7):901-913. [doi:10.1061/(ASCE)GT.1943-5606.0000057]

Lee, S.Y., 1990. Centrifuge Modelling of Cone Penetration Test in Cohesionless Soil. PhD Thesis, Cambridge University, UK.

Luong, M.P., Touati, A., 1983. Sols grenus sous fortes contraintes. *Revue Francaix de Geotechnique*, **23**:51-63 (in French).

Mair, R.J., Wood, D.M., 1987. Pressuremeter Testing: Methods and Interpretation. CIRIA Ground Engineering Report, In-situ Testing, Butterworths, London.

Randolph, M.F., Dolwin, J., Beck, R., 1994. Design of driven piles in sand. *Geotechnique*, **44**(3):427-448. [doi:10.1680/geot.1994.44.3.427]

Salencon, J., 1969. Contractionquasi-statique d'une cavité a symétrie sphérique ou cylindrique dans un milieu elastoplastique. *Annales des Ponts et Chaussées*, **4**:231-236 (in French).

Salgado, R., Lyamin, A.V., Sloan, S.W., Yu, H.S., 2004. Two and three dimensional bearing capacity of foundations in clay. *Geotechnique*, **54**(5):297-306. [doi:10.1680/geot.54.5.297.46720]

Schofield, A.N., 2005. Disturbed Soil Properties and Geotechnical Design. Thomas Telford, London, p.142.

Shepard, D., 1968. A Two-Dimensional Interpolation Function for Irregularly-Spaced Data. Proceedings of the ACM National Conference, p.517-524. [doi:10.1145/800186.810616]

Tatsuoka, F., Sakamoto, M., Kawamura, T., Fukushima, S., 1986. Strength and deformation characteristics of sand in plane strain compression at extremely low pressures. *Soil and Foundations*, **26**(1):65-84.

Terzaghi, K., Peck, R.B., 1948. Soil Mechanics in Engineering Practice. John Wiley, New York.

van den Berg, P., 1994. Analysis of Soil Penetration. PhD Thesis, Delft University of Technology, Delft, the Netherlands.

Yasufuku, N., Hyde, A.F.L., 1995. Pile end-bearing capacity in crushable sands. *Geotechnique*, **45**(4):663-676. [doi:10.1680/geot.1995.45.4.663]

Yu, H.S., Mitchell, J.K., 1998. Analysis of cone resistance: Review of methods. *Journal of Geotechnical and Geoenvironmental Engineering*, **124**(2):140-149. [doi:10.1061/(ASCE)1090-0241(1998)124:2(140)]

Zhou, J., Deng, Y.B., Ye, J.Z., Jia, M.C., 2009. Experimental and numerical analysis of jacked piles during installation in sand. *Chinese Journal of Geotechnical Engineering*, **31**(4):501-507 (in Chinese).